

ADVENTURES IN HIGH INTENSITY ACOUSTIC TESTING: A LOUDSPEAKER SYSTEM FOR SMALL-SCALE TESTS

J Hargreaves Acoustics Research Centre, University of Salford, UK
J Hipperson Funktion One Research, UK
D Wong-McSweeney Acoustics Research Centre, University of Salford, UK
N O'Doherty Acoustics Research Centre, University of Salford, UK

1 INTRODUCTION

In the space and aerospace industry, there is a need to perform High Intensity Acoustic Testing (HIAT). This aims to recreate in the laboratory, for the purpose of qualification testing, the extreme acoustic environments that designs must survive in use, for example, that a satellite can withstand the noise of rocket launch and reach orbit without damage. HIAT has become a mandatory part of the space-launch pre-flight testing process and is stipulated in launcher manuals for all payloads.

Traditionally such tests have been performed in giant reverberation chambers, driven by gas-powered electro-pneumatic noise sources mounted on giant horns. But these facilities are extremely expensive and rare, so since the mid-1990s there has been growing interest in using loudspeakers to generate the sound field. This has the notable advantage that the test system can be brought to the test article, which can be highly advantageous since it's far easier to transport loudspeakers than a spacecraft.

This technology is known as Direct Field Acoustic Noise (DFAN) testing within the industry, so called because the intention is that the direct sound field from the loudspeakers – which are relatively close – dominates over the reverberant sound from the enclosing room. Nonetheless, the aim remains to subject the test article to a diffuse sound-field, being a chaotic field in which acoustic waves arrive from every direction with equal energy. This is chosen to ensure that any possible pattern of excitation which the test article might be especially sensitive to is included in the exciting sound field, i.e., it always includes the worst case, and provides equivalence with reverberant tests. It is achieved in DFAN via special control algorithms that feed multiple groups of loudspeakers different 'drive' signals and ensure the sound-field meets both the prescribed Sound Pressure Level (SPL) target and a target for incoherence between signals captured at the control microphones. A comprehensive review of this technology can be found in the 2022 literature review in ref. 1.

There are a small number of specialist companies who supply DFAN systems commercially. These are typically very large, both because of the need to surround a large test article, and because of the number of transducers needed to achieve the required sound power density. But there is also a market for HIAT testing of smaller components, which the commercial test labs of the University of Salford has been servicing for several years. This case study paper stems from an effort to develop this into a turnkey testing service, using loudspeakers developed by Funktion One Research Ltd.

Section 2 details the test requirements, the control system and loudspeaker configurations tested. Section 3, then presents some findings that are not commonly reported in the literature: loudspeaker electroacoustic efficiency, condition monitoring via electrical impedance, & mutual acoustic coupling. Finally, section 4 draws conclusions, surmises lessons learned, and suggests some areas where further research is required in the future.

2 TEST REQUIREMENTS AND CONFIGURATIONS

2.1 Standardised Test Requirements

The main principles and requirements for DFAN testing are reviewed in chapter 2 of ref. 1. Test requirements are typically stated as a set of target third-octave band SPLs, plus a lower threshold that must be exceeded in all bands in order for the test to be valid, and an upper abort threshold.

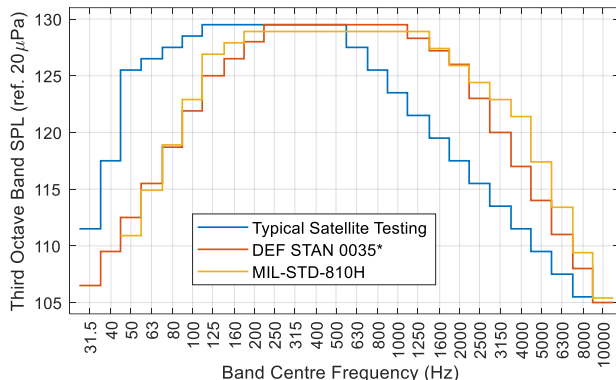


Figure 2: Target Third Octave Band SPL Profiles adjusted to 140dB OASPL.



Figure 2: 24 in 6 out Siemens SCADAS Mobile Front-end / Controller with Vibco

In the space-launch domain, test procedures are specified in standards and handbooks such as NASA-STD-7001b, NASA-HDBK-7005 and ECSS-E-HB-32-26A, while the SPL profiles themselves are given in launcher manuals. These standards are clearly written with reverberation chamber testing in mind, e.g., they state minimum distances between the test article and other hardware (control mics, noise sources, chamber walls) that are incompatible with DFAN operating principles. But the literature shows DFAN tests are equivalent and caveats allowing DFAN are appearing in later revisions. Further information specific to DFAN is given in NASA-HDBK-7010 and an ESA handbook is in preparation. An SPL profile typical for satellite testing is shown in blue in Figure 2, though its Overall SPL (OASPL) has been adjusted to be 140dB ref. 20µPa, slightly lower than typical launcher requirements.

In addition to the satellite testing requirements reviewed in ref. 1, there are also military HIAT requirements, which are standardised in DEF STAN 0035 (UK) and MIL-STD-810H (US). These are again focussed on reverberation chamber testing, but MIL-STD-810H contains caveats allowing DFAN. These profiles have no absolute level but are instead relative to a prescribed OASPL that may vary with application. They are shown in orange and yellow in Figure 2 (note DEF STAN 0035 contains no target SPL so the profile shown is the mean of the upper and lower thresholds).

Comparing these, it is clear that the satellite testing requirement is far more ‘bass-heavy’, whereas the bulk of the energy in the military standards is between 250Hz and 1kHz. Satellite tests are also quite short – rarely more than 1 minute – whereas military test durations extend up to several hours.

2.2 Control System

DFAN systems require special controllers in order to hit both their SPL and diffusivity targets. Their operating principles and history is summarised in chapter 4 and appendix A4 of ref. 1. A Siemens SCADAS Mobile was used for these tests (Figure 2), including the required Vibration Control (Vibco) module – DFAN control algorithms are descended from shaker control – running with the MIMO Random Control Workbook in TestLab v2206. Control was typically from 40Hz to 10kHz running at 3.125Hz FFT resolution – an accepted choice for DFAN – meaning over 3000 frequencies were individually controlled. Eight ¼” GRAS 46BG high SPL microphone sets were used.

All HIAT control algorithms use multiple control microphones so are Multi-Input (MI). Additionally, DFAN requires multiple shaped noise signal ‘drives’ to achieve a diffuse field, hence the controller is Multi-Input Multi-Output (MIMO). This is in contrast to controllers for reverberation chambers, which are typically Multi-Input Single-Output (MISO). These were used in early attempts at DFAN in the 1990s but shown to be inadequate. Arguably, DFAN matured in the late 2000s when MSI and Spectral Dynamics transferred MIMO control technology from shakers to acoustics¹.

Figure 3 compares MIMO and MISO control in our test configuration #3 (detailed in section 2.3.3). Four drives were used for the MIMO case. It can be seen that both methods achieved an average Power Spectral Density (PSD) across microphones (black) that is close to the target (green), but that

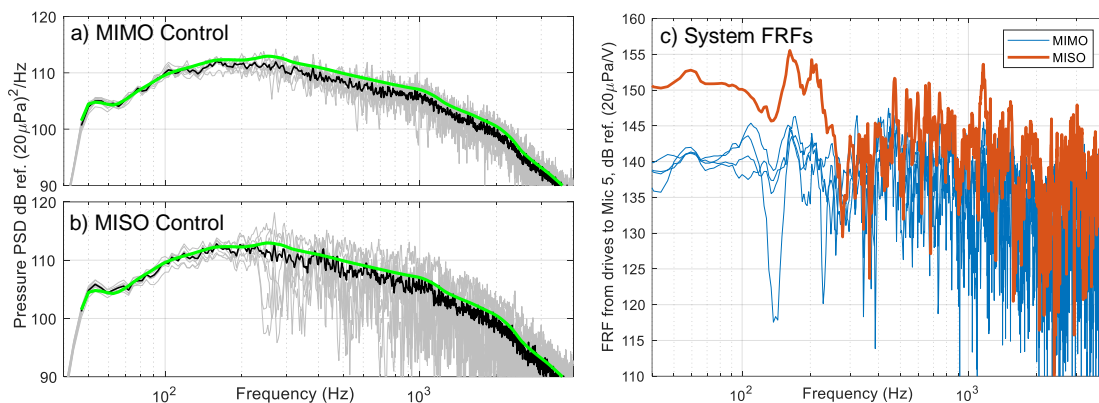


Figure 3: Effects of MIMO versus MISO control. Left: Power Spectral Density during a 139dB OASPL test with the DEF STAN 0035 spectra with a) MIMO control, and b) MISO control. Right: Measured system FRFs from the various drives to Mic 5, for both control schemes.

the spread of individual mic PSDs (grey) is far greater with MISO control than with MIMO. This indicates that under and over testing will occur at some positions with MISO control even if the average PSD is on target. Figure 3c shows the Force Response Functions (FRFs) from the drives to mic 5 (chosen arbitrarily) for both cases. MISO has a reputation for being more power efficient than MIMO, and it can be seen that the FRF is around 12 dB higher at low frequencies. However, this is only the expected gain from four times as many speakers being connected, and above 250Hz it experiences a notch – so is less efficient – and then becomes quite irregular. The peaks and notches are likely modal effects, which the MISO system has no means of suppressing. In contrast, the MIMO controller can adjust the relative coherence and phase of its drives to suppress modes that produce high variance of SPL or reduce diffusivity. The principal of this is explored in ref. 2.

Either 7 or 8 microphones were designated as control mics for these tests. In a commercial test, more ‘monitor’ microphones would also be used, but here insufficient were available. The Siemens control algorithm requires more control mics than drives, so anything from 5 upwards is allowed. But some artefacts were seen with 5 and 6 control mics that did not occur when using 7 or 8.

2.3 Loudspeaker Configurations

In a departure from normal DFAN practice, it was decided to run the tests in a small reverberation chamber at the University of Salford Acoustics Test Laboratories. This was mainly due to availability and logistics – it is advantageous to use a room that is acoustically isolated – and followed the precedent set by previous tests. It was also hoped it might increase SPL by adding ‘room gain’. Four pilot test campaigns were run, each with different loudspeaker configurations, as reported below.

Previous testing had suggested that modern COTS concert sound subwoofers have sufficient power density to be used for DFAN tests. The barrier then is primarily the mid-high loudspeakers, which in concert sound prioritise fidelity over raw power, and are too large, meaning they lack the required output power density.

To address this requirement, Funktion One Research Ltd designed and manufactured several prototype ‘HIAT610’ devices. These comprised a 2x3 array of compact horn cells each loaded with a high-power 10” loudspeaker optimised for upper bass and midrange reproduction. Since overheating is known to be a limitation in DFAN tests¹, these incorporated thermal management features on the rear of the unit to dissipate the heat generated by the loudspeaker motor (Figure 4). This was not necessary with the subwoofers as all the designs used have the loudspeaker oriented with the motor facing outwards.



Figure 4: Exterior view of thermal management features on rear of a HIAT610 cell

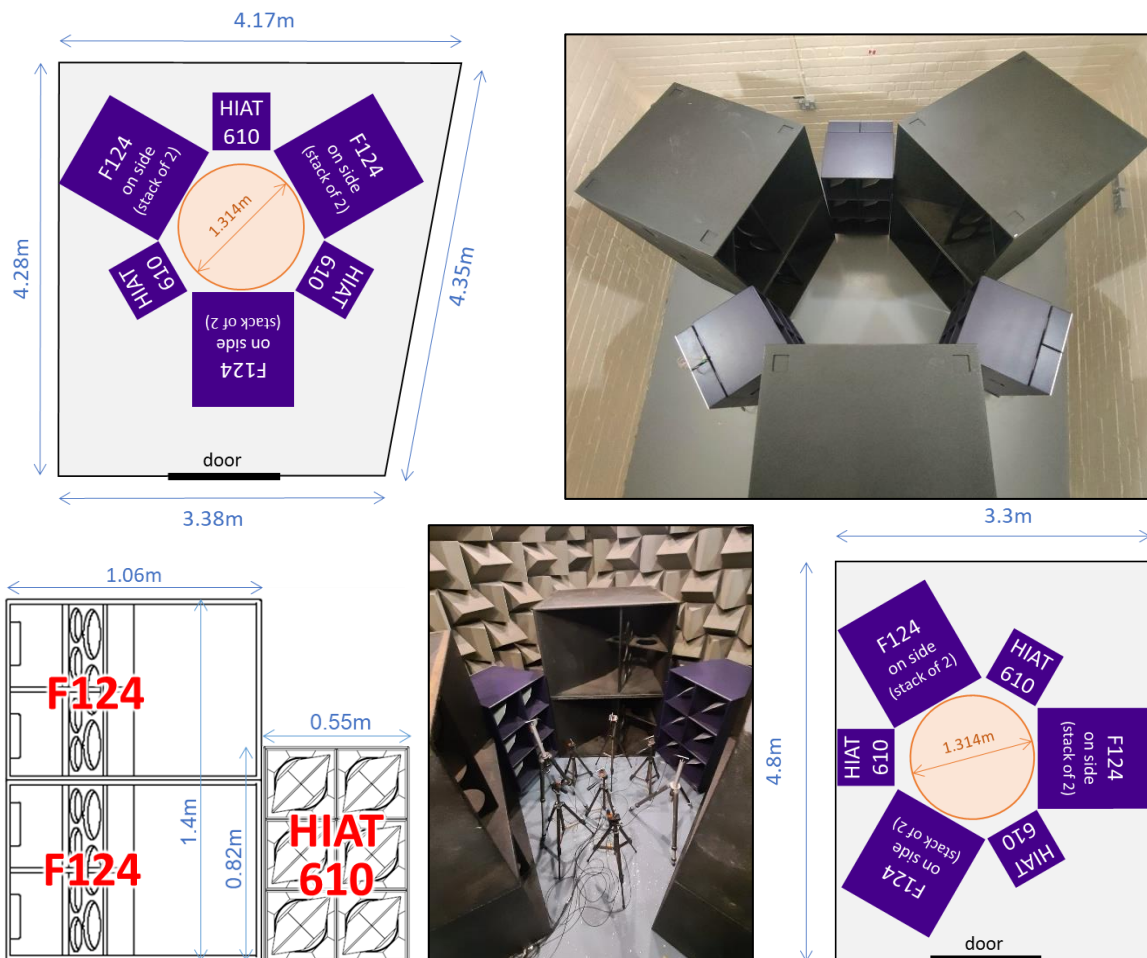


Figure 5: Test configuration 1. Top row plan view and photograph (without cables or mics) in the small reverberation chamber. Bottom left: elevation view, with cabinet sizes for comparison. Bottom right: plan view and photograph (with one HIAT610 removed) in the hemianechoic room.

2.3.1 Test 1: Three HIAT610 and Six F124

This first test configuration was conceived to address the satellite testing profile (blue line in fig. 1). This is bass heavy, so the three available HIAT610s were complemented by six Funktion One F124 enclosures, each featuring a dual-coil 24" loudspeaker. Three drives were used, each feeding one HIAT610 and a pair of F124 – note that the MIMO control software requires all drives to be full-range. The crossover between these was varied in the region of 200-300 Hz, sometimes with some (deliberate) overlap. Processor delays were applied to time-align the paired loudspeakers.

Initial tests feeding the system with a single pink noise signal achieved a sustained 147dB OASPL. Tests with the satellite target profile and the MIMO controller achieved 143dB OASPL for 1 minute.

The tests were repeated in both the small reverberation chamber and a hemianechoic chamber to assess the room gain provided by the former. This was found to be less than expected, with the maximum achievable hemianechoic OASPL being only about 2dB lower. The explanation for this is two-fold: i) the loudspeakers turned out to be quite effective electroacoustic absorbers, causing the reverberation time in the reverberation chamber to drop significantly once they were installed; ii) the closed nature of the loudspeaker array means it supports its own mini reverberant field, as has been anecdotally reported by other DFAN operators. This was clearly audible when working in the hemianechoic chamber, and meant the rate of energy escape was not as high as anticipated.

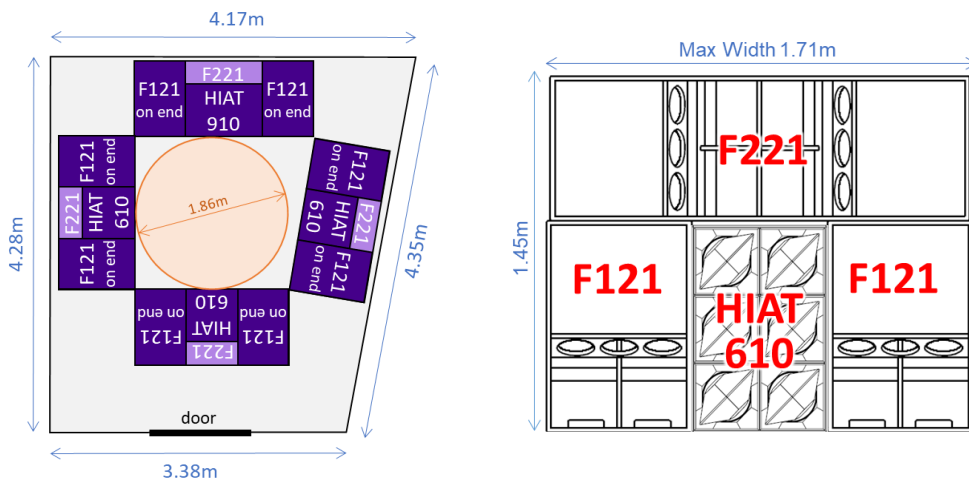


Figure 6: Test configuration 2 in the small reverberation chamber. Left: plan view. Right: stack elevation (exception is stack #1, which has a HIAT910 in place of a HIAT610).

2.3.2 Test 2: Four HIAT610, eight F121 and four F221

Two limitations of test 1 were that: i) the loudspeaker combination was not optimised for the less bass heavy military test profiles, and ii) that the testing arena was too small. For test 2, the F124s were switched to a mixture of F121 and F221 21” loudspeakers, which were expected to be more efficient at higher frequencies and are shallower, allowing a larger test arena as shown in Figure 6.

Four drives were used for this test. Only three HIAT610 were available at this point, so an older prototype – here termed a ‘HIAT910’ – was also used. This comprised a 3x3 array of the same horn cells, but with loaded with an older transducer design and lacking thermal management features. This made one stack wider, leading to a slight asymmetry in the otherwise square test arena.

The maximum OASPL sustained with this configuration was 139dB. 140dB was possible, but only for about 20 seconds, after which amplifier limiters engaged and the SPL target was not met. This reduction compared to test configuration #1 was thought to mainly be because of the increased distance from the loudspeakers to the control mics, a feature necessary to satisfy the standards.



Figure 7: Test configuration 3. Left: stack elevation. Right: Photo with one stack removed. Stack in centre of photo again has HIAT610 substituted with the HIAT910, making it wider.

2.3.3 Test 3: Four HIAT610, eight F215, eight F121, and four F221

To try and increase the maximum OASPL compared to test 2, test 3 added eight F215 15" loudspeakers, the main operating band of which sits between that of the F221 and the HIAT610. They are conveniently similar in size to the HIAT610, easing arraying (Figure 7). The total rated loudspeaker power was now 20.8kW, powered by 32kW of rated amplifier power.

An advantage of the new configuration was that the HIAT610s were raised off the floor, allowing the same to be done with the test article, as standards require. A Perspex plate was included as a vibroacoustic test article (Figure 8), monitored by accelerometers connected to the SCADAS. This was suspended on shock cords in line with DEF STAN 0035.



Figure 8: Test arena in config 3. Note the mics are elevated to match the HIAT610s.

However, despite the added 6.4kW of extra power added by the F215s since test 2, the maximum sustainable OASPL remained at 139dB. This level was achieved in a more stable manner and with less problems with amplifier limiters interacting badly with the controller, and the added F215s meant the configuration was far superior on the DEF STAN 0035 profile. But even 140dB OASPL could only be achieved for 20-30 seconds before power compression reduced the loudspeaker electroacoustic efficiency to the point where limiting amplifier levels were required to maintain the SPL target. It is thought that this lack of SPL increase, despite added input power, was due to further increased absorption in the room. Subjectively, it was no longer reverberant. Additionally, at these SPLs the brickwork of the chamber moves a discernible amount, which will cause additional losses.

2.3.4 Test 4: Four HIAT610, eight F215 and eight third-party dual 18" cabinets

It was realised during test campaign 3 that the F221s were not being worked hard by the DEF STAN 0035 profile yet were likely causing quite significant absorption. For this fourth and final set of pilot tests the aim was to replace these with another eight F215s, making sixteen in total, but these could not be sourced so instead a set of eight third-party dual 18" cabinets were used. Serendipitously, these proved to have a phase response that was very compatible with the F215s once time aligned.

Another change was that the tests were moved to the laboratory's large reverberation chamber, the idea being that this should be less affected by absorption from loudspeakers and therefore retain more 'room gain'. This unfortunately turned out not to be the case and, despite extensive repositioning over many trials, the 139dB OASPL limit persisted. Considering this, the system would ideally have then been run in the small reverberation chamber, but a technical fault meant this was not possible.

An interesting result was that the long reverberation time in the large chamber caused the controller to exceed its SPL targets. The same phenomenon occurs if using the HIAT610s alone in the small chamber. This is likely due to the room impulse response exceeding the length of the FFT frame used by the controller. Noise generated in previous frames is still reverberating in subsequent frames, where it is viewed by the analyser as incoherent noise from another source. The control algorithm does not account for this, hence an SPL response a few dB over the target curve occurs.

2.4 Evaluation of these pilot tests

These tests showed the Funktion One loudspeaker system offers a robust solution for High Intensity Acoustic Testing. They also showed the effectiveness of the Siemens MIMO controller, which controlled the SPL tightly and repeatably with no issues from modal activity evident. Except for test 4 in the large reverberation room, the average SPL always met target and appeared very uniform. Higher OASPLs would have been desirable, and development will continue to try and increase this.

3 FINDINGS

The majority of DFAN papers mainly show third octave plots of the achieved SPL, since this is evidence that the required test profile was achieved and the environment the test article was exposed to constitutes a valid test. Here, however, we will concentrate on other results that reveal more about the performance of the loudspeakers. Section 3.1 considers electroacoustic conversion efficiency, section 3.2 reports on condition monitoring via electrical impedance, and section 3.3 reports findings on mutual acoustic coupling between speakers, a phenomenon we found to be significant, but which is not mentioned in the DFAN literature.

All of these tests require high resolution current and voltage data to be acquired at the output of the amplifier. While many amplifiers monitor loudspeaker impedance as a slowly updated single value, observing variation over frequency or with a time resolution that allows voicecoil temperature variation to be inferred requires much faster rate data. To the best of our knowledge, the only amplifier platform that offers this feature is from Powersoft, but there currently offer limited options for exporting data out of the amplifier for postprocessing. So, we instead measured these quantities using a 16 channel Dewesoft Sirius system. The single channel measurements were taken with their proprietary high current (<20A) and high voltage (<200V) sensing adaptors. The multichannel measurements we taken using an array of transformer-isolated current and voltage adaptors that were developed in-house and verified against the Dewesoft ones.

Dewesoft X software was setup to provide a live monitoring view, but the data herein has been computed from the raw time histories in Matlab. Auto and cross power spectral densities were computed using Welch’s method with a 4,096 sample FFT, 32 averages and Hamming windows with 50% overlap. The sampling rate was 20kHz. Real electrical power is found from the real part of the cross power spectral density between voltage and current, which was then integrated to give third octave band levels where required. Impedance was computed using a H1 estimate.

3.1 HIAT610 Electroacoustic Efficiency

The primary mode of failure in transducers in DFAN is voicecoil overheating. Since the cause of this is electrical power flowing through the voicecoil, and the objective is maximum acoustic power output, it follows that maximising electroacoustic conversion efficiency will lead to maximum achievable SPL.

To measure acoustic conversion efficiency in a realistic way, the sound power output by a HIAT610 device was measured in the small reverberation room following ISO 3743-1:2010, with electrical input power measured as described above. After performing the averaging required by the standard, the acoustic output power is divided by the electrical input power to obtain the electro-acoustic efficiency. The same test was repeated for a conventional 2-way 12”+1” loudspeaker, a Funktion One F1201, for comparison. Figure 9 shows both results.

Notably the horn loaded HIAT610 is around 10dB more efficient than the conventional loudspeaker in the 160Hz to 500Hz range. Efficiency here is close to 20% and peaks at 30% at 250Hz, an extra-ordinarily high figure that showcases Funktion One’s transducer design and horn loading technology.

(Notes: a higher efficiency figure for the ARS Neutron is claimed in ref. 3, but the details of its measurement are unclear. The efficiency spike of the 1201 at 125Hz is thought to be an anomaly most like caused by room modes – the sound power measurement has high uncertainty at this low frequency.)

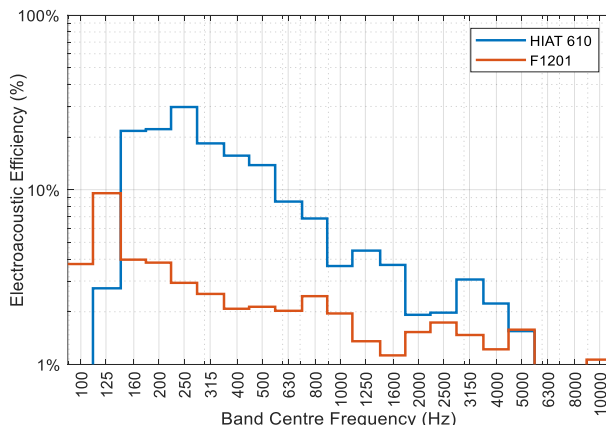


Figure 9: Electroacoustic efficiency of a HIAT610 compared against a bass reflex design (an F1201)

3.2 Conditioning Monitoring via Electrical Impedance

Plots of electrical impedance versus frequency give valuable insight into the properties of a loudspeaker, both its own electro-mechanical properties and its radiation loading. The latter property is exploited in section 3.3. But here the objective was to infer voicecoil temperature. After observing how numerous live impedance plots changed as power compression kicked in, it was inferred that the portion of the curve above the mechanical and fundamental horn resonance, but below the rise due to inductance, was the part most strongly governed by resistance due to heating. The resistance in this range was averaged to give the plots below; 600Hz – 1kHz for a HIAT610, and 300Hz – 800Hz for an F215. Voicecoil temperature $T(t)$ was inferred from resistance $R(t)$ using the linear model:

$$T(t) = T_{ref} + [R(t) - R_{ref}]/\alpha R_{ref} \tag{1}$$

Here R_{ref} was the (cold) resistance at the start of the test, T_{ref} was taken to be 25°C, and the thermal resistance coefficient α was taken to be $3.9 \times 10^{-3} \text{ } ^\circ\text{C}^{-1}$. Thermocouples were also used to measure the magnet and heatsink temperatures but – while informative for longer tests – these react far too slowly to show voicecoil temperature due to the large thermal mass of the magnet.

Figure 10 shows electrical input power, resistance and inferred temperature for four HIAT610 and four F215 during a 2-minute 139dB OASPL test with the DEF STAN 0035 profile in configuration 3. Note that only six drivers were connected in the HIAT910 unit, so its data is comparable. The test starts with three 10 second build-up steps – 130, 133 & 136 dB – before the full 139 dB section starts. Impedance and inferred voicecoil temperature can be seen to rise as soon as the power is applied, rising most steeply at the start of the 139dB section, and following an exponential profile typical of a first-order system, as is expected for thermal mass. This rise in resistance reduces electroacoustic conversion efficiency, and the controller responds by increasing input power to maintain the SPL at the target, which then causes impedance to rise further & the cycle continues. F215 1 shows reducing drive power after 1 minute, which is almost certainly due to amplifier limiting. Again, the controller will respond by increasing drive voltage, a vicious cycle that – once it occurs – quickly drives the amplifier inputs into clip and causes a test to have to be halted. This lack of integration between controller and amplifier is a key shortcoming of current DFAN control systems. It is also evident that the controller may push some drives harder than others, an undesirable effect that the user cannot control.

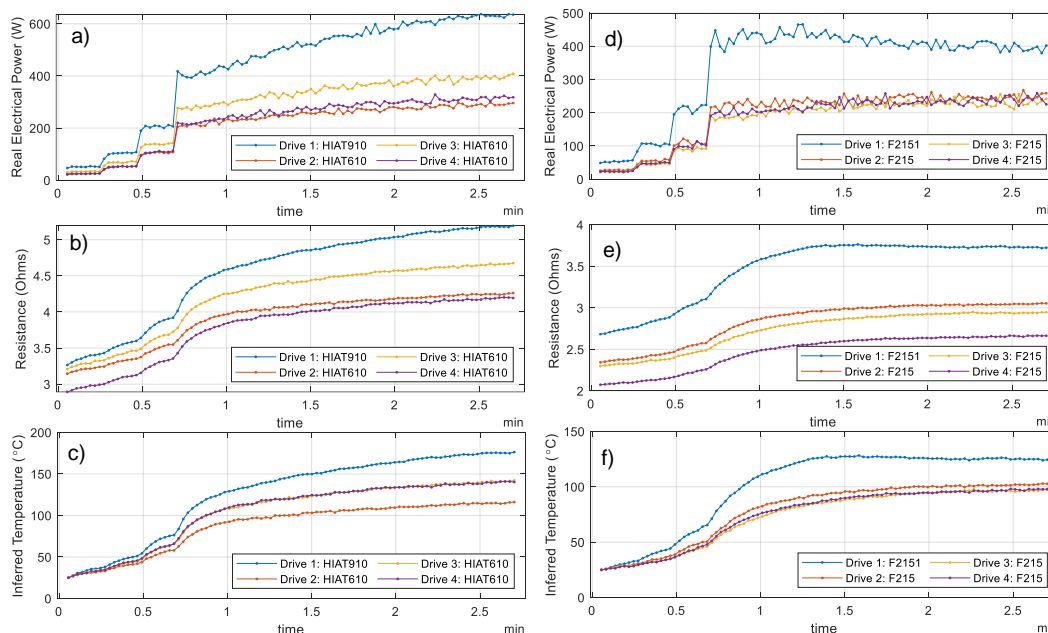


Figure 10: Power (top), resistance (middle) and inferred voicecoil temperature (bottom) of four HIAT610 (left) and F215 (right) on the drives of a 139dB DEF STAN 0035 test in configuration 3.

This gradual reduction in acoustic efficiency is why DFAN tests at the highest achievable levels are always short in duration. That is sufficient for satellite launch applications because those tests are short (since the loudest part of rocket launches is also quite short), but military standards may require much longer durations up to several hours. But reducing OASPL by merely 3 or 6 dB can prevent this cycle, meaning the system reaches equilibrium and allowing those longer test periods to be achieved.

In these longer tests, amplifier power supply limiting can also be a constraining factor, causing SPL to fall below target even when loudspeaker impedance is stable. This was observed 10 minutes into a 130dB OASPL test and could be seen in the power and impedance measurements, with the former cycling in a sawtooth pattern and impedance following it subject to the thermal integration time. This class D amplifier, which was rated 2kW per channel for music, was unable to maintain even a quarter of that power with continuous random noise, ultimately leading to it being replaced by a unit of even higher power. That modern amplifiers have power ratings based on their burst current is well known, but this experience highlights how their stated power ratings are meaningless for DFAN applications. The maximum injected electrical power in Figure 10 – which is spread over six 10” drivers in the HIAT610 and two 15” drivers in the F215 – is also well below their power rating for music.

Figure 11 uses the same processing to investigate the benefits of the thermal management features of the HIAT610 in a longer duration test. The blue line is from a horn cell with the thermal management features shown in Figure 4, while the orange one is the same horn and loudspeaker but with a standard wooden backbox. Here a pink noise generator of constant RMS voltage was used, so the impedance rise causes a reduction in SPL, which is also shown. The right column of figures shows the same data as the left but zoomed in on the first 3 minutes. Note that Figure 10 is for six horn cells wired in parallel, whereas the data in Figure 11 is for a single cell, hence the very different resistance and power scales. The pink noise excitation was high pass filtered at 200Hz.

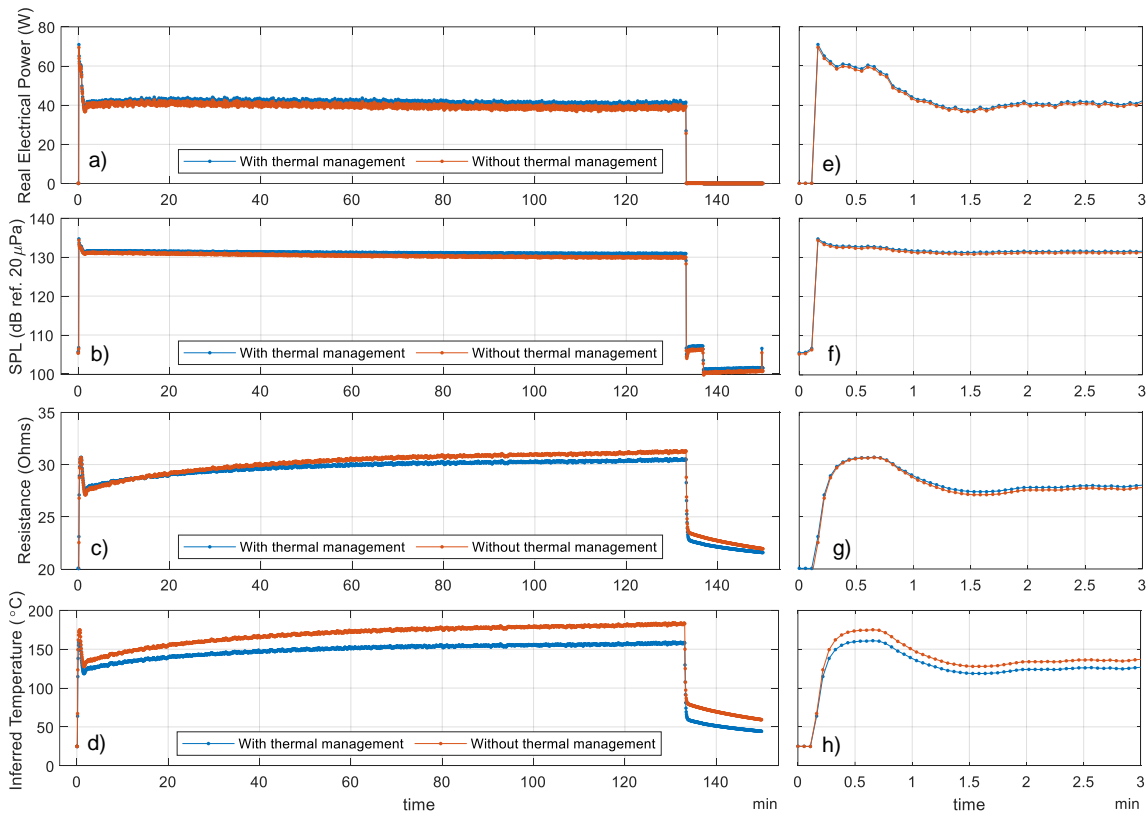


Figure 11: Comparison of a single 10” horn cell with (blue) and without (orange) thermal management features. a&e: Electrical input power; b&f: Achieved SPL; c&g: Resistance; d&h: inferred voicecoil temperature. a-d: full time history, e-h: first 3 minutes.

It can be seen from the plots in the right column that voicecoil temperature and resistance rises very quickly once the power is applied. This is due to the very small thermal mass of the voicecoil itself, and it is identical on both units since the thermal management has not been able to have any effect yet. SPL peaks at 134dB but then quickly reduces to 131dB due to the rise in impedance. This shift is the threshold that the ‘toaster test’ method for maximum power output in section 5.3 of AES2-2012 specifies, hence it seems that this input power – 40W – is a suitable limit for this driver. Notably, AES75-2022 gives power ratings more meaningful for music, but AES2 seems well suited to DFAN.

Temperature and resistance reach equilibrium around 30 seconds in. This is due to the thermal mass of the loudspeaker magnet sinking the heat from the voicecoil and is again the same in both cases. Then, around 30-90 seconds, there is a drop in applied input power; this is thought to be due to amplifier power supply limiting. After this, all quantities stabilise, but the long-term plots in the left-hand column show that impedance and voicecoil temperature are continuing to rise. Now the thermal management begins to make a difference. The temperature of the driver in the wooden box increases more dramatically because it has no means of dissipating the heat it is generating. But the unit with the thermal management features can dissipate this heat, leading to its voicecoil being 25°C cooler at the end of the test. This difference is not very large, but the heating effect is cumulative so will become important on longer tests. The thermal management features also decrease cool-down times, which is important when running multiple short tests. Thermocouple measurements showed the metal black plate of the unit with thermal management was at 70°C. The driver in the wooden box was sufficiently hot that the thermocouple had detached, and it was making a discernible burning smell.

3.3 Mutual Acoustic Coupling

The results in section 3.2 show the potential of impedance measurement as a tool for condition monitoring. But performance differed when this was used during full tests. Figure 12 shows why.

Coherence between input voltage and current for a HIAT610 or F215 run alone (solid lines) is close to 1 for all frequencies where there is significant input signal, decreasing below the corner frequency of the drive’s high pass filter.

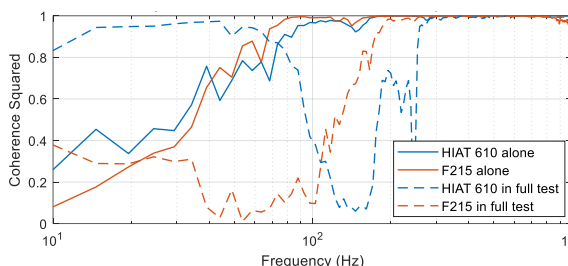


Figure 12: Coherence between voltage and current measurements for a HIAT610 (blue) and an F215 (orange) when measured alone (solid) and in a HIAT test configuration (dashed).

But when the same measurements are taken in a full system with multiple drives active, the coherence trend is quite different (dashed lines). Now it drops off at a much higher frequency, below which current and/or voltage must be corrupted by incoherent energy from another drive (note that it was validated that this wasn’t due to cable crosstalk). This is another reason why the average resistance values in figures 10 and 11 were averaged over a frequency range higher than this. More intriguingly, the HIAT610 (blue dashed line) shows coherence between voltage and current at frequencies below the range where the drive signal is present. This can only be due to it acting microphonically in response to other energy in the chamber, presumably the F221s, based on the frequency range.

To investigate this in a more controlled way, voltage & impedance were measured for three scenarios in the hemianechoic chamber: a) a single HIAT610 alone; b) 2 HIAT610 facing away from each other; c) 2 HIAT610 facing towards each other 1.86m apart, matching their separation in test configurations 2 and 3. In b and c, the second unit was either: i) muted, ii) fed from the same noise generator as the first unit, making them coherent, or iii) fed from a different noise generator, making them incoherent. Additionally in case c, the second unit was unplugged from its amplifier and instead either its: iv) open-circuit voltage, or v) short-circuited current, was measured to assess the microphonic effect.

Figure 13 a&b show the resistance and reactance measured on the first unit for case a (blue line), and case b (green, orange and yellow lines respectively showing the second unit muted, driven coherently, and driver incoherently). For the undriven case c.i (muted, green) there is little difference from case a (alone, blue). The results from case b (facing away) are not shown because they also

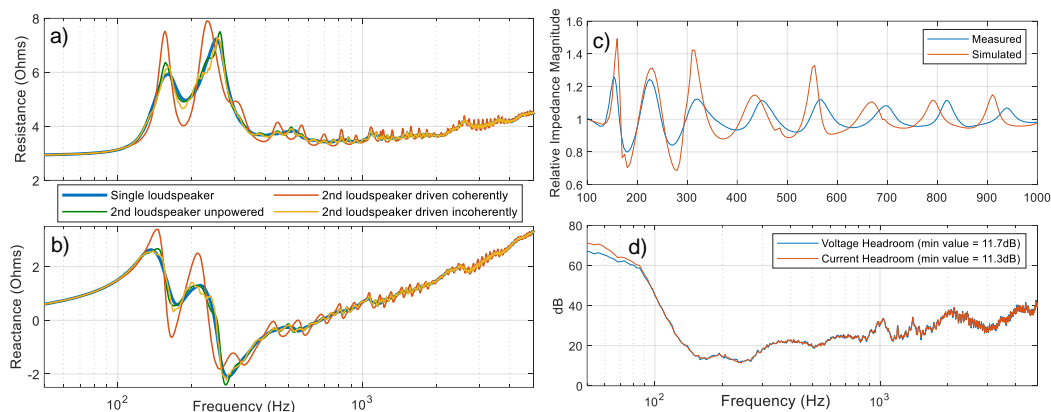


Figure 13: Resistance (a) and reactance (b) of a HIAT610 alone (blue), or with a second unit 1.86m away that is unpowered (green), driven coherently (orange) or incoherently (yellow). c) Relative changed in impedance of driven unit – measured (blue) and simulated with FEM (orange). d) Headroom in dB between drive power in one unit and microphonic effect in another.

showed little difference from a. When the second unit is driven incoherently (c.iii, yellow) there is some difference, but it is quite subtle. But case c.ii, where the second unit is fed the same signal, shows a drastic difference. This changes the resonance peaks and notably leads to periodic peaks and troughs in the impedance curves, the spacing of which can be roughly related to the spacing of the loudspeakers – including the horn length – compared to wavelength.

This correlation couldn't be proven exactly, however, so a numerical model was created to validate the effect. This used a lumped parameter model of the loudspeaker, coupled to a Finite Element Method (FEM) model of the horn interior, coupled to a Boundary Element Method (BEM) model of the box exterior and surrounding air, all implemented in COMSOL Multiphysics. Symmetry was exploited to reduce computational cost while capturing the symmetry of the device and the floor reflection. Case c.ii was simulated efficiently by adding a further symmetry plane at $0.93\text{m} = 1.86\text{m} / 2$. This models a single unit firing at a sound hard wall, which is equivalent according to the image source principle.

The Thiele-Small parameters of the loudspeaker driver were only known approximately, so the simulated impedance curve was not expected to exactly match the measured one, and it did not. So instead, the ratio of the impedance from case c.ii to case a was computed, which normalises out most of the model tuning issues while still showing the difference due to acoustic coupling. This trend is shown for both measurement and simulation in Figure 13c, where a very similar trend is seen. Phase isn't shown because it was negligible. The difference in peak spacing is probably due to the lack of model tuning perturbing the driver reactance, which will detune the eigenmodes causing this effect.

Finally, Figure 13d shows the measured microphonic effect. The power in this is shown as ratio in dB compared to the power of the signal from the amplifier driving the primary loudspeaker. This coupling is very strong, leading to power in the receiving voicecoil that only 12dB lower at some frequencies. Interestingly, the minimum value is roughly the peak efficiency from Figure 9 squared (applied once for radiation and then again for microphony) and converted to dB. This is unlikely to be enough to cause serious issues for an amplifier driving this second loudspeaker. But it shows that firing a large number of loudspeakers towards each other into a cavity, as DFAN does, is very different from using them separately or firing them in different directions, as is more commonplace in concert sound.

4 REFLECTIONS AND CONCLUSIONS

The pilot tests reported in this paper yielded both successes and frustrations. A lot of lessons were learnt along the way, which we have attempted to share herein. Overall, the tests were successful, and we now have a reliable and well-benchmarked test service that can be offered commercially. The MIMO controller operated as billed, nullifying chamber modes, but struggled in a reverberant field.

The main frustration was that the maximum OASPL achieved was not higher. Commercial DFAN systems have been achieving 147dB OASPL for around a decade, but it should not be forgotten that those systems have always been far larger, with an order of magnitude more transducers and amplifier power brought to bear.

It was also notable how abrupt the limit due to power compression is. This is often stated anecdotally, but to witness it first-hand was revealing. It also makes it easier to understand why it took the DFAN industry a decade to get from 147dB OASPL to 150dB, as has been achieved by recent proprietary loudspeaker systems. This is only 3dB, but that is still double the acoustic and electrical power! Once it occurs, a vicious cycle begins, and system components rapidly move outside their optimal zone.

Related to this, it became apparent that the lack of integration between amplifiers – and/or impedance-based condition monitoring – and the controller is a serious gap in current DFAN technology. Limiting is essential to protect loudspeakers, but it increases system non-linearity and interacts extremely badly with the control algorithm, leading to spiralling conditions that require tests to be aborted. If instead the limiting could be communicated to the controller, then more intelligent action could be taken. Limiters were also observed to cause ‘pumping’ effects that can be damaging to drivers.

This requires more than a communication back-channel. The MIMO control algorithm needs to be extended to also factor the power output to different drives into its calculations, such that a need to limit certain drives can be integrated. This would also prevent some drives from being asked to deliver far more power than others, as was seen in some results herein. Finally, it may also allow crossover filters to be integrated into the controller, which would mean different drives could have different frequency ranges. With this, all loudspeaker groups could be fed independently, eliminating the need for separate crossovers and time-alignment. A possible route to this end might be to add Tikhonov-style regularisation to the (squared) system matrix inversion (surmised in appendix A4 of ref. 1).

From a practical perspective, it was seen that amplifier and loudspeaker power ratings for music are meaningless in DFAN applications. It was also seen that absorption from loudspeakers is significant, as is mutual coupling and microphonic effects. Notably, the latter appears to be more significant in loudspeakers that are horn loaded to maximise radiation efficiency, since the effects are reciprocal. Furthermore, this shows that the radiation load seen by a loudspeaker in a DFAN application is quite different from that experienced in a concert sound application, which further reinforces the conclusion from ref. 1 that proprietary DFAN designs are essential. Acoustically, it was observed that loudspeaker arrays support their own reverberant field, and that modes include the loudspeaker internals and mechanical compliance. Basing modes on the geometry of their external boundary, as was done in ref. 2 and its references, is not adequate when the speakers are horn loaded.

5 ACKNOWLEDGEMENTS

The authors would like to acknowledge the contribution of Pete Rollinson of AudioServ Ltd, who provided the majority of loudspeakers and amplifiers and contributed to system setup and tuning.

6 REFERENCES

1. J. A. Hargreaves, ‘Literature review of Direct Field Acoustic Noise (DFAN) testing’. Technical Report, University of Salford, 2022. <https://doi.org/10.17866/h20g-8587>.
2. J. A. Hargreaves, ‘Analysis and Control of Acoustic Modes in Cylindrical Cavities with application to Direct Field Acoustic Noise (DFAN) Testing’. Proc. Internoise, Glasgow, 2022. <https://salford-repository.worktribe.com/output/1324217>
3. D. Schick et al, ‘Verifying a Novel Approach to Acoustic Testing: Acoustic Devices & Control Systems’. Proc. 32nd Aerospace Testing Seminar, Virtual, 2021.